Microelectronics Reliability 97 (2019) 79–84

Contents lists available at ScienceDirect

Microelectronics Reliability

journal homepage: www.elsevier.com/locate/microrel

An observation and explanation of interior cracking at the interface of solder by electromigration

Qizhi Wang[a], Qingyi Liu[a], Zheng Zhang[a], Min Miao[b], Yehao Su[c], Fei Su[a,*]

[a] School of Aeronautical Science and Engineering, Beihang University, Beijing, China
[b] Beijing Information Science & Technology University, Beijing, China
[c] College of Electrical and Information Engineering, Hunan University, Changsha, China

ARTICLE INFO

Keywords:
Electromigration (EM)
Interfacial crack
Solder
Reliability

ABSTRACT

The electromigration (EM) of a solder joint under high-current stressing causes damage and reduces its service life. Previous studies have suggested that EM-induced cracks typically initiate at the cathode corner where the electron current enters, and propagate across the intermetallic compound and solder interface. Herein, however, another type of propagation is experimentally demonstrated whereby cracks initiate from voids located in the middle of the interface and propagate in two directions. This phenomenon was investigated further with finite element simulations. These simulations showed that, when the solder corners become rounded via the wetting phenomenon that occurs during solder reflow, the current density around the voids is greater than that at the solder corner. Under these conditions, cracking will initiate from the side of an existing void, instead of the corner from where electron current flows into the solder ball, when tensile stress is present at the void and compressive stress at the electron current entrance.

1. Introduction

The pursuit of miniaturization and high performance in the microelectronics industry has led to a significant increase of the current density in packaging technology, where the average current density in solder joints has reached 10^4 A/cm^2. As a consequence, electromigration (EM) has become inevitable in electronic packaging and causes new failure modes. Therefore, the reliability of solder balls under EM has become a vital area of research.

A typical failure mode of solder joints under current stressing is the initiation and propagation of pancake-type void/crack along the interface of the intermetallic compound (IMC) and solder at the cathode. In most of the available reports on EM induced crack via EM, crack usually initiates from the solder corner where the current density concentration occurs [1–5], as shown in Fig. 1. What's more, empirical formula used to estimate the mean time to failure (MTTF) was developed based on this assumption [6,7]. However, in our and a few other's experimental investigations [8], voids/cracks initiated from locations other than solder corners were found, this observation deviated from the traditional knowledge on failure behavior and the MTTF estimation of solder by EM.

From the view of failure analysis and reliability evaluation, it is necessary to investigate the mechanism of this special failure mode. As demonstrated in the existing work [9–11], we believe both stress and electron current density play important role in the EM failure of solder, and we try to reveal this problem with the relevant theory.

2. Experimental

2.1. Preparation for experiments

To explore the EM behavior of a solder bump under current stressing, the following specimens were carefully designed and fabricated.

2.1.1. Printed circuit board design

We design the EM samples with two different printed circuit board (PCB) specimen designs for the top and bottom as PCB-A and PCB-B, which are shown in Fig. 2. The PCB-A was made of Rogers ceramic and the PCB-B was made of FR4, whose coefficients of thermal expansion are 17×10^{-6} and 35×10^{-6} C^{-1}, respectively. A 50 μm-thick layer of solder mask was deposited on the copper films and traces of PCB-A and PCB-B, where upon 162 copper pads with 0.2 mm in diameter were uncovered by the solder mask. Subsequently, 162 commercial-grade SnAg3.5Cu0.5 (SAC) solder balls were manually attached to these Cu pads with the aid of sticky solder paste. After reflow, the solder balls were planted on both the upper and lower PCBs and a circuit loop was

* Corresponding author.
E-mail address: sufei@buaa.edu.cn (F. Su).

https://doi.org/10.1016/j.microrel.2019.04.013
Received 7 December 2017; Received in revised form 15 December 2018; Accepted 23 April 2019
Available online 03 May 2019

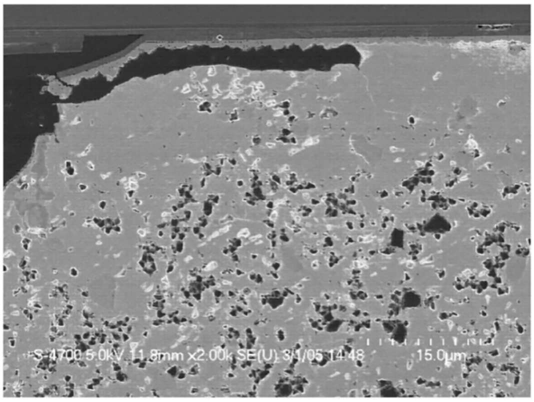

Fig. 1. SEM image of the void formation in a flip chip 95.5Sn-4.0Ag-0.5Cu solder bump (from Ref. [1]).

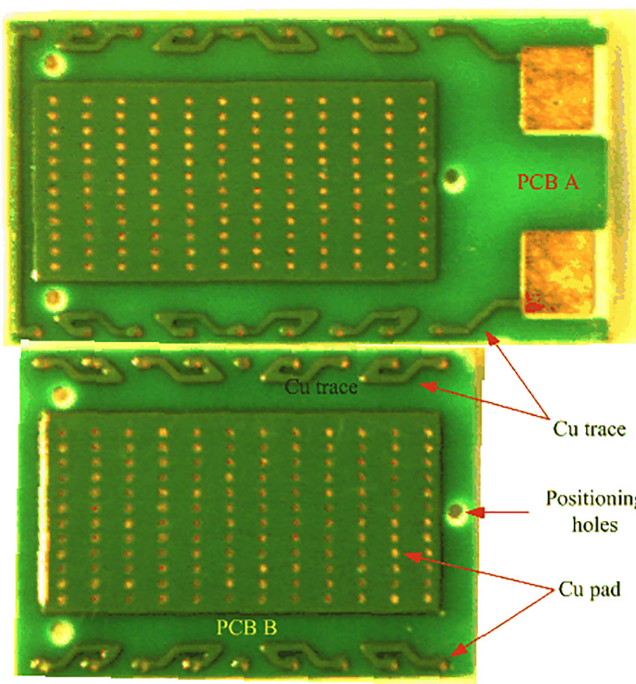

Fig. 2. Photograph of the specimen designs for the EM test, showing PCB-A (upper) and PCB-B (lower).

made.

It should take notice of the fact that only the solders along the array edges of PCB-A and PCB-B were connected in the electrical loop. The other 144 solder balls in the internal region of the PCB arrays were blind, whose sole purpose were to provide mechanical support to maintain the shape of the solders. Because of the special design of the copper trace, the electron current flowed into the solder from one corner (i.e., the entrance) and flowed out from the diagonally-opposite corner (i.e., the exit).

2.1.2. Solder specimen preparation

The solder specimens were processed with a grinding and polishing machine so that half of the solder balls were polished off and the largest cross-sectional view was exposed. A direct current (DC) up to 2.5 A was then applied to the solder balls in series, corresponding to an average current density scale of 10^4 A/cm^2, and in situ observations of EM-induced damage of the solder joint was carried out under SEM.

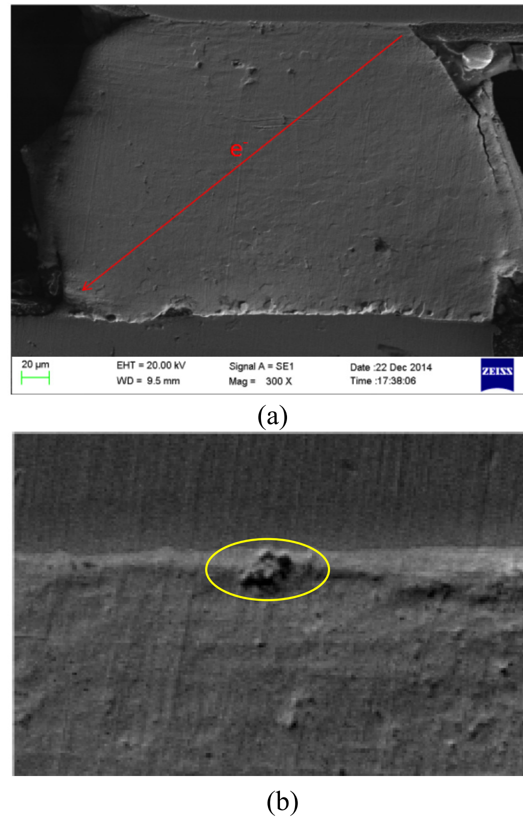

Fig. 3. SEM images of the solder at the initial stage of EM testing showing the (a) overall morphology and (b) local morphology of a void induced by air trapping.

2.2. Experimental results and discussions

Fig. 3 shows the original morphology of a solder joint where some small voids are seen at the interface of the IMC and solder, and a typical void is shown in Fig. 3(b). This kind of defect is inevitably induced by air trapping during reflow [8], but its role in the failure of solder under current stressing was usually underestimated.

Initially, we focused our attention on the cathode corner of the solder joint as in typical EM experiment. No cracking was observed in the solder after 156 h of current stressing, as shown in Fig. 4. It was not until 204 h later of current stressing, cracking was observed. However, it did not occur at the corner of solder, but at the end of void circled in Fig. 4. The void expanded to about 20 μm in length, exhibiting a more slender appearance with two increasingly sharper ends, as shown in Fig. 5. As the EM process proceeded during the following 39 h, the voids expanded rapidly along the interface and met cracks formed by other voids. As shown in Fig. 6, this expansion and combination created obvious crack throughout the entire cathode interface, which resulted in complete failure of the solder joint.

Compared with other specimens, the experimental result of this specimen (Figs. 5 and 6) has two notable features: first, the nucleation position of the crack was the void at the interface rather than the typical corner location. Second, the life-time of the solder joint was far shorter than the others. Regarding the first notable feature, we speculate that the current density of the corner location was reduced owing to the conduction angle formed during the reflow process and the thick copper pad. As a result, the current density at the corner was even smaller than that at the two ends of the void, especially after the EM resulted in sharper ends on the void. Regarding the second notable feature, we believe that more than one void might exist at the interface and expanded simultaneously, which would accelerate the progress to break

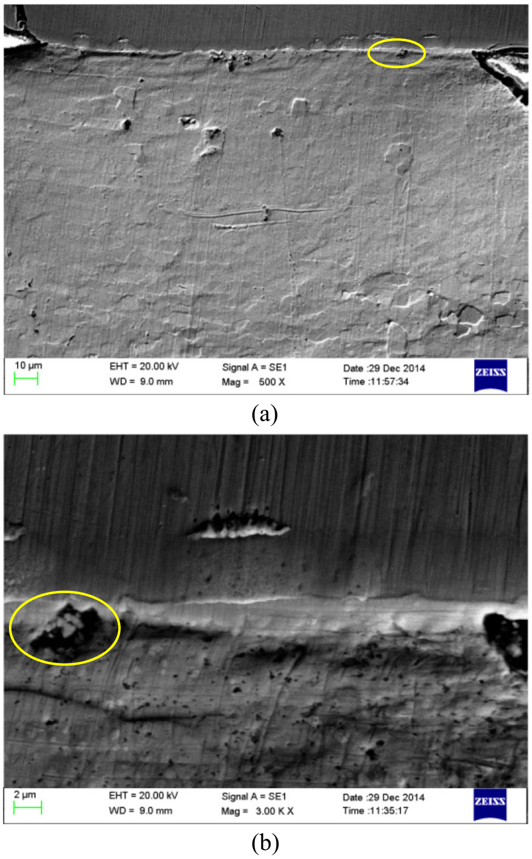

Fig. 4. SEM image of the crack after 156 h of EM without expanding. (a) a void therein (yellow circle), and a more magnified view of the same void (b). (For interpretation of the references to colour in this figure legend, the reader is referred to the web version of this article.)

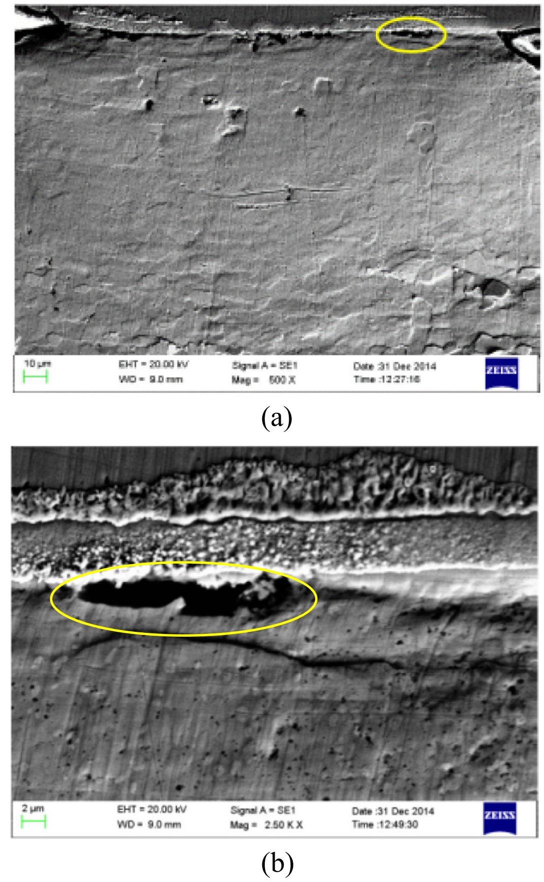

Fig. 5. SEM image of the crack after 204 h of EM with a short length of the void, showing a low-magnification view of the interface (a) and a void therein (yellow circle), and a more magnified view of the same void (b). (For interpretation of the references to colour in this figure legend, the reader is referred to the web version of this article.)

the solder under EM. In the following sections, we will confirm these conjectures using the finite element (FE) method and compare the differences of vacancy concentrations at the two locations, i.e. the corner of solder joint and the two ends of the pancake like void.

3. Finite element modeling

3.1. Governing equations of EM

Electromigration is considered to be a mass diffusion that can be characterized by closed system equations wherein a vacancy is the token of migration [12–14]. Herein,

$$\int_{v}\left(C_{v0}\frac{\partial c}{\partial t}+\nabla\cdot\mathbf{q}-G\right)dV=0 \tag{1}$$

where C_{v0} is the equilibrium concentration of vacancies in stress free field; c is the normalized vacancy concentration, $c = C_v/C_{v0}$, where C_v is the vacancy concentration; t is time; q is the vacancy flux vector; and G is the vacancy generation/annihilation rate.

Neglecting the temperature gradient in a specimen, the vacancy flux q is controlled by the single driving force, i.e., the electron wind, and by two counter flows, i.e., the density gradient and stress gradient, given as

$$\mathbf{q}=-D_vC_{v0}\left[\nabla c+\frac{Z^*e}{kT}(-\rho\mathbf{j})c+\frac{cf\Omega}{kT}\nabla\sigma_{\text{spherical}}\right] \tag{2}$$

where D_v is the vacancy diffusivity; Z^* is the vacancy effective charge number; e is the electron charge; ρ is the metal resistivity; j is the current density vector; f is the ratio of the atomic volume to the vacancy volume; Ω is the atomic volume; k is the Boltzmann constant; T is the absolute temperature; σ_{ij} is the stress tensor and $\sigma_{\text{spherical}} = (\sigma_{11} + \sigma_{22} + \sigma_{33})/3$ is the spherical stress (including external stress and stress induced by EM). The coupling effect of multi-physics field induced by EM can be described using Eq. (2).

For simplicity, linear elasticity is presupposed as an intrinsic mechanical property of SAC solders. The total strains existing in solders include the mechanical elastic strain components $\varepsilon_{ij}{}^{e}$ and the inelastic strain components induced by EM, such that $\varepsilon_{ij}{}^{\text{electromigrationcan}}$

$$\varepsilon_{ij}=\varepsilon_{ij}^{e}+\varepsilon_{ij}^{\text{electromigrationcan}} \tag{3}$$

and the inelastic strain components satisfy

$$\frac{\partial\varepsilon_{\text{trace}}^{\text{electromigrationcan}}}{\partial t}=\Omega C_{v0}(f\nabla\cdot\boldsymbol{q}+f'G),$$
$$f'=1-f \tag{4}$$

Thus, the elastic stresses will be

$$\sigma_{ij}^{e}=S_{ijkl}(\varepsilon_{kl}-\varepsilon_{kl}^{\text{electromigrationcan}}) \tag{5}$$

where S_{ijkl} is the stiffness matrix. The force equilibrium without body forces should be

$$\frac{\partial\sigma_{ij}}{\partial x_j}=0 \tag{6}$$

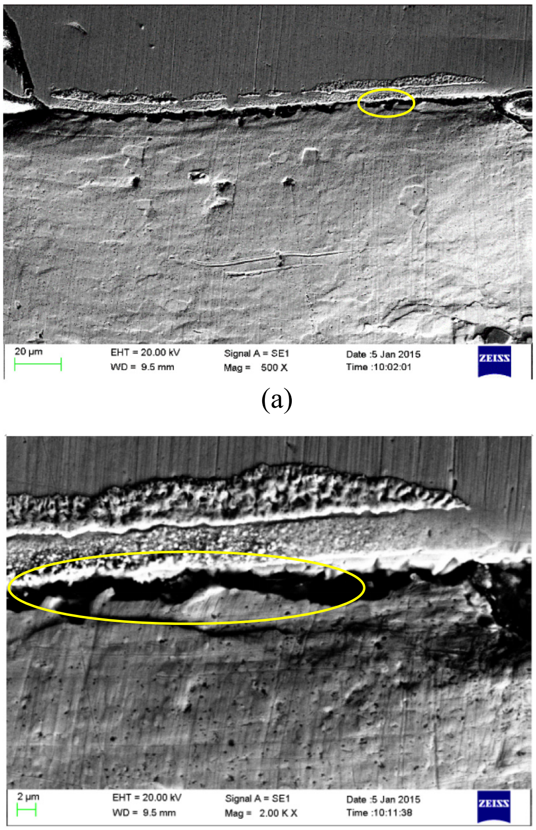

Fig. 6. SEM topograph of the solder joint in Fig. 4 after 243 h of EM, showing a low-magnification view of the interface (a) and the void therein (yellow circle), and a more magnified view of the same void (b). (For interpretation of the references to colour in this figure legend, the reader is referred to the web version of this article.)

3.2. Finite element (FE) simulation of vacancy concentration and its variation

We established a two-dimensional FE model based on the solder in Fig. 3, according to the actual structure and size. It should be noted that the corner of the solder was round with radius 0.02 mm instead of sharp, which is a result of wetting during solder reflow. This helped to significantly reduce the current density and stress concentration at the corner of the solder joint. On the other side, an elliptical cavity with long axis of 0.007 mm and short axis of 0.0028 mm was used to represent the void, equivalent radius at the two corners is 0.0035 mm.

A single cell was modeled as shown in Fig. 7, which includes the Cu pads/traces of PCB-A and PCB-B sandwiching the solder ball. Periodic boundary conditions were then supposed for this single cell, wherein 0 V and 600 A/mm^2 were applied to the top right and bottom left corners of the solder, respectively.

As a failure index in the theoretical studies, the vacancy concentration was studied at the electron current entrance (cathode) and the crack. Two steps were involved in the FE simulation: In the first step, a current density and thermal stress owing to solder reflow were simulated. In the second step, the mesh of the model was held unchanged and the EM-induced vacancy and its variation with time were simulated, wherein the electron current density and thermal stress simulated in the first step were used as the initial conditions of the second step.

The ABAQUS thermo-mechanical module was employed in the second step during this simulation. However, the Jacobian matrix and the residual vector must be redefined based on the principles of the FE method, and the vacancy concentration must be introduced as a new degree of freedom instead of the temperature. User subroutines were therefore developed to implement this matrix redefinition and substitution, it also implemented the external thermal stress to the model as initial condition, more details can be found in ref. [8]. The thermal, electrical, and mechanical properties of the SAC and Cu materials employed in the FE model are listed in Table 1.

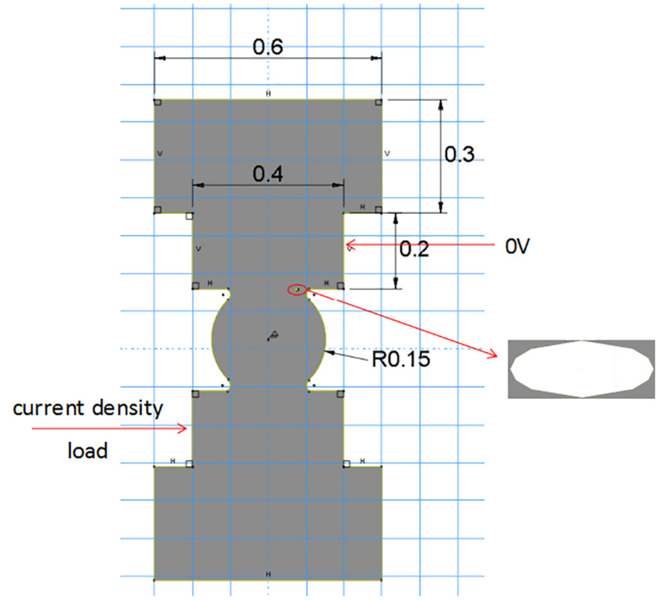

Fig. 7. Geometry of the single cell model used for the FE simulation, showing the electrical boundary condition at the solder corners and geometry of the void at the interface.

The solder itself was assumed to be a closed system, wherein the interfaces between the SAC solder and the Cu pad (i.e., Cu_6Sn_5 and Cu_3Sn) would be a blocking boundary for the vacancy diffusion. Such a model has been previously adopted to simulate EM-induced plastic deformation and stress [17] successfully.

3.3. Simulation results and discussions

Fig. 8 shows the simulated current density and thermal stress field of the solder, respectively. It can be seen that the current density was highly concentrated at the tips of void (1568A/mm^2) rather than the corner of solder (567A/mm^2). Similarly, Fig. 9 shows the thermal stress of solder, in this case, the stresses at the tips of void (left: 59.6/right: 65.3/MPa) are also higher than that at the solder corner (−58.7 MPa) where electron current enters.

Table 1
Parameters of the SAC solder and Cu traces/pads used for FE simulation [15,16].

		SAC	Cu
T	Absolute temperature (K)	298	–
E	Young's modulus (GPa)	30	120
ν	Poison's ratio	0.36	0.34
k	Boltzman's constant (J/K)	1.38×10^{-23}	–
D_v	Average vacancy diffusivity (cm^2/s)	1×10^{-4}	–
Z^*	Effective vacancy charge number	1.5	–
C_{v0}	Equilibrium (cm^{-3})	6.66×10^{13}	–
ρ_{SAC}	Resistivity (ohm·cm)	1.15×10^{-5}	–
Ω	Volume of atom (cm^3)	2.71×10^{-23}	–
f	Average vacancy relaxation factor	0.6	–
τ_s	Relaxation time of vacancy (s)	0.0018	–
κ	Electrical conductivity (1/Ω·mm)	7519	57,143
α	Expansion (CTE × 10^{-5}/K)	2.45	1.7

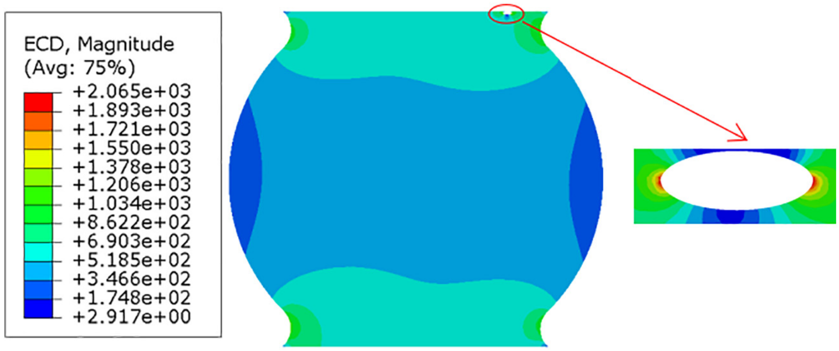

Fig. 8. Simulation results of the electrical current density field in the solder. (Inset) Current density field in the region of the void.

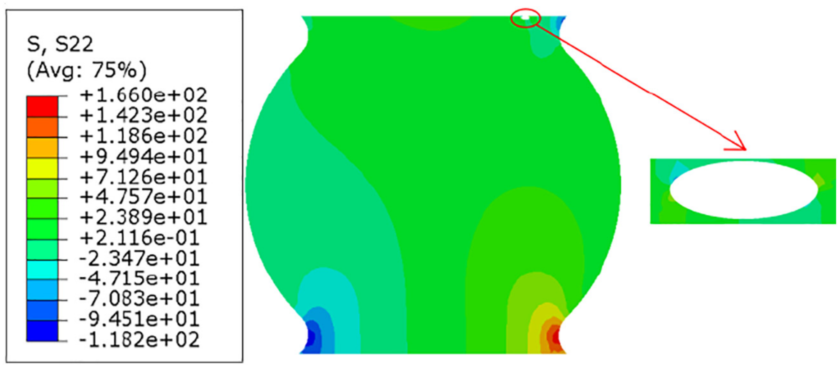

Fig. 9. Simulation results of the thermal stress field in the solder after cooling from 125 to 25 °C (rigidity of solder above 125 °C was neglected).

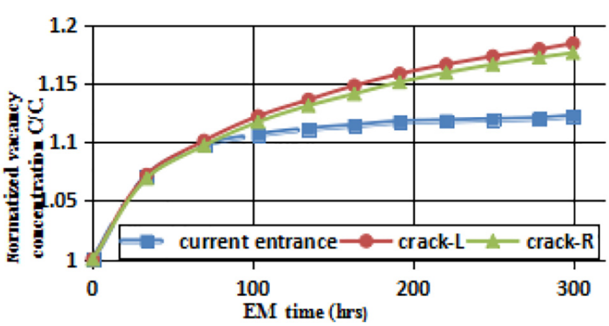

Fig. 10. Time-evolved vacancy concentration in the solder at the locations of the electron current entrance (cathode) and at both crack ends (crack-L and crack-R).

Variation of vacancy concentration was adopted as the reference to evaluate the rate of electromigration. The evolution of the local vacancy concentration as a function of time at three locations (i.e., the electron current entrance and the two tips of the void) are plotted in Fig. 10. It can be seen that the evolution behavior and data of the local vacancy concentrations at the two void tips are very similar; both increase faster than that at the electron current entrance. For example, if a normalized vacancy concentration of 1.15 was set as the local failure criterion [18], the void will get expanded at 168 h and 189 h, respectively (please note the experimental data is 156 h). As a contrast, the local vacancy concentration at the cathode end is just 1.12. These simulation results explained why EM induced failure occurs first at the void tips rather than the cathode corner.

In the above simulation, only one void was adopted. Definitely, there maybe more than one void appear at the interface of solder and copper pad. They may have mutual influence on the stress field and electrical density field. We take two identical voids in the FEM model to investigate their influence on the EM behavior of solder. In the model, the size and position of one void was kept the same as in the previous models, but another one was set to the left of it with different distances.

Simulation results of stress field and electrical current density filed under different gap of voids are examined. It was found that, only when their gap decreased to less than 0.013 mm and 0.003 mm, respectively, mutual influence on current density field and thermal stress field

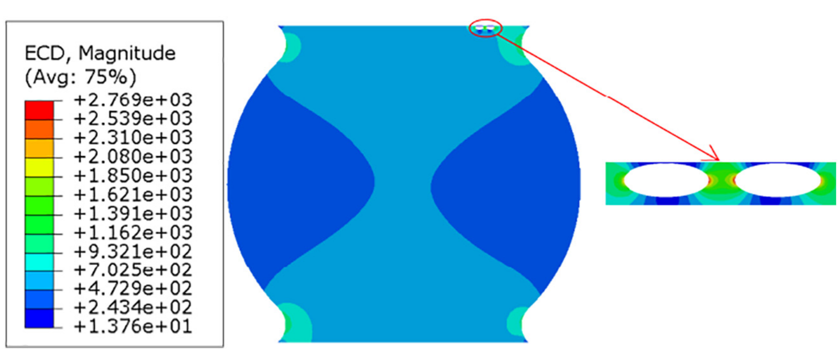

Fig. 11. Simulation results of the electrical current density field in the solder. (Inset) Current density field in the region of two voids (gap of voids is 0.002 mm).

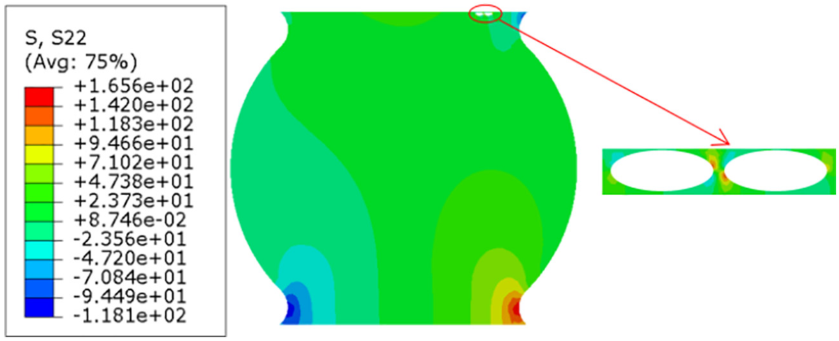

Fig. 12. Simulation results of the thermal stress field in the solder after cooling from 125 to 25°C (gap of voids is 0.002 mm).

became obvious. Simulation result of electrical current density under the void gap of 0.002 mm was shown in Fig. 11, where the current density at the neighbouring tips of voids is about 2330A/mm^2. The simulated thermal stress at the same location is shown in Fig. 12, where stress at the neighbouring tips of voids is about 90.1 MPa. It can be concluded that, when the gap of voids is beyond 0.013 mm, existence of more than one voids will not have obvious influence on the crack initiation life of solder by EM, however, they will accelerate the crack expansion rate and thus shorten EM life of solder.

4. Conclusions

Although the corner of the solder joint where electron current enters is generally the focus of stress and current density, and thus electromigration and the earliest crack nucleation are most likely to occur here, some exceptions may occur. In this experiment, a void was identified at the interface of a solder joint and the IMC, from which a crack initiated to expand throughout the entire interface, ultimately leading to failure of the ball. To some extent, this discovery may subvert people's understanding to some extent; During the reflow process, some air bubbles may be trapped in the solder and cause voids, the tips of the voids may be even sharper than that of the solder corner. With the aid of finite element simulation, we found the current density, stress and the vacancy concentration which is usually an indicator of damage at tips of the void are greater than that at the corner of the solder joint, therefore, the crack appears and expands the very earliest at this void location. At the same time, our theoretical model predicts that when the thermal stress was compressive at the electron current entrance and tensile at the void tips, the above phenomenon is more obvious. The existence of more than one voids will not influence the crack initiation life of solder by EM if their gap is far enough, but may accelerate the crack expanding rate. In conclusion, our research provided theoretical and experimental evidence for the failure analysis of solder joints and the design of high-reliability solder joints.

Acknowledgement

The authors express their gratitude to the financial support of Natural Science Foundation of China with grant number 11372024 and 11672340, at the same time, this work was also supported in part by the Importation and Development of High-Caliber Talents Project of Beijing Municipal Institutions (Great Wall Scholar, No.CIT&TCD20150320).

References

[1] L. Zhang, S. Ou, J. Huang, et al., Effect of current crowding on void propagation at the interface between intermetallic compound and solder in flip chip solder joints [J], Appl. Phys. Lett. 88 (1) (2006) 012106.
[2] K. Yamanaka, Y. Tsukada, K. Suganuma, Studies on solder bump electromigration in Cu/Sn–3Ag–0.5 Cu/Cu system[J], Microelectron. Reliab. 47 (8) (2007) 1280–1287.
[3] E.C.C. Yeh, W.J. Choi, K.N. Tu, et al., Current-crowding-induced electromigration failure in flip chip solder joints[J], Appl. Phys. Lett. 80 (4) (2002) 580–582.
[4] P. Dandu, X. Fan, Assessment of Current Density Singularity in Electromigration of Solder Bumps[C]//Electronic Components and Technology Conference (ECTC), 2011 IEEE 61st, IEEE, 2011, pp. 2192–2196.
[5] O. Taner, K. Kijkanjanapaiboon, X. Fan, Does current crowding induce vacancy concentration singularity in electromigration?[C]//Electronic Components and Technology Conference (ECTC), 2014 IEEE 64th, IEEE, 2014, pp. 967–972.
[6] P. Su, M. Ding, T. Uehling, et al., An Evaluation of Electromigration Performance of SnPb and Pb-Free Flip Chip Solder Joints[C]//Electronic Components and Technology Conference, 2005. Proceedings. 55th, IEEE, 2005, pp. 1431–1436.
[7] I.A. Blech, Electromigration in thin aluminum films on titanium nitride[J], J. Appl. Phys. 47 (4) (1976) 1203–1208.
[8] K.L. Lin, S.M. Kuo, The electromigration and thermomigration behaviors of Pb-free flip chip Sn-3Ag-0.5 Cu solder bumps[C]//Electronic Components and Technology Conference, 2006. Proceedings. 56th, IEEE, 2006(6 pp).
[9] Z. Zhang, Q. Liu, et al., Influence of stress on the electromigration life of solder[J], IEEE Trans. Compon. Packag. Manuf. Technol. 7 (5) (2017) 762–767.
[10] Zhi-Hao Zhang, Xi-Shu Wang, Huai-Hui Ren, Su Jia, Hui-Hui Yang, Simulation study on thermo-fatigue failure behavior of solder joints in package-on-package structure, Microelectron. Reliab. 75 (2017) 127–134.
[11] Huai-Hui Ren, Xi-Shu Wang, Su Jia, Fracture analysis on die attach adhesives for stacked packages based on in-situ testing and cohesive zone model, Microelectron. Reliab. 53 (2013) 1021–1028.
[12] Michael Pecht, Kailash C. Kapur, Rui Kang, and Shunong Zhang, "Foundations of Reliability Engineering", May 2011.
[13] M. Lin, C. Basaran, Electromigration induced stress analysis using fully coupled mechanical and diffusion finite element analysis with non linear material properties [J], Comput. Mater. Sci. 34 (1) (2005) 82–98.
[14] M.E. Sarychev, V. Zhinikov Yu, General model for mechanical stress evolution during electromigration[J], J. Appl. Phys. 86 (6) (1999) 3068–3075.
[15] H. Ye, C. Basaran, D.C. Hopkins, Deformation of solder joint under current stressing and numerical simulation–I[J], Int. J. Solids Struct. 41 (18–19) (2004) 4939–4958.
[16] C. Basaran, M. Lin, Electromigration induced strain field simulations for nanoelectronics lead-free solder joints[J], Int. J. Solids Struct. 44 (14–15) (2007) 4909–4924.
[17] F. Su, Z. Zhang, Y. Wang, et al., Study of Electromigration-induced stress of solder [J], J. Electron. Packag. 137 (2) (2015) 021006.
[18] S.N. Wang, 3D finite Element Simulation for Solder Joint Electromigration in IC Chip[D], Zhejiang University of Technology, Zhejiang, 2007.